

Supplementary information

Chirality of the Rhodamine Heterodimer Linked to DNA Scaffold: An Experimental and Computational Study

P.S. Rukin^{a,}, K. G. Komarova^{a,†}, B. Fresch^b, E. Collini^b, F. Remacle^a*

^aTheoretical Physical Chemistry, UR MolSys B6c, University of Liège, B4000 Liège, Belgium

^b Department of Chemical Sciences, University of Padova, via Marzolo 1, 35131 Padova, Italy

* present address: Federal Scientific Research Centre “Crystallography and Photonics” Photochemistry Center, Russian Academy of Sciences, ul. Novatorov 7a, Moscow, 119421 Russian Federation

† present address: The Fritz-Haber Center for Molecular Dynamics and The Institute of Chemistry, Safra Campus, The Hebrew University of Jerusalem, Jerusalem 91904, Israel

Table of contents

1. Experimental methods.....	2
2. Structures of the supramolecular complexes via MD simulations (Figs. S1-S2)	3
3. Solvation shells for RHO and TAMRA units from MD simulations (Fig. S3)	4
4. Intermolecular angles and coupling between the monomers (Fig. S4).....	5
5. Averaging of the profiles	7
6. Absorption and CD properties of the bare dimers in solution (Table S1 and Fig. S5).....	8
7. Distributions for the intermolecular angles in the D and <i>ch</i> -D isomers (Figs. S6-S7)	9
8. Typical structure for the excited state computation (Fig. S8).....	11
9. The dominant natural transition orbital pairs (Fig. S9).....	12
10. Structures with spurious electronic transitions	13
11. Spectra averaged over localized and delocalized transitions (Figs. S10-S13).....	14
12. Oscillator strength for the S ₀ -S ₁ transition (Fig. S14).....	17
13. Scheme of the optical isomerisation	18
14. Table of the coordinates of the bare dimers.....	19

1. Experimental methods

Sample preparation. The sequences of the oligonucleotides in the studied samples were suitably designed to lead to a strongly coupled dimer configuration upon self-assembly of the double helix. The final synthesis was commissioned to Integrated DNA Technologies that provided the oligonucleotides with HPLC purity grade.

GTG AAC ACT CTA GG-TAMRA
CAC TTG TGA GAT CCC TGA CAC CTA CAC C
RHO-G ACT GTG GAT GTG G

The samples were prepared dissolving the oligonucleotides in water at pH=7.5 (HEPES buffer). The final concentration of the dyes was 25 μ M. Simulated melting curve analysis confirmed that at 25 °C the yield of the hybridized product is higher than 99%.

Linear characterization. The linear absorption spectra were recorded using a Varian Cary 5 UV-visible-NIR spectrophotometer. Circular Dichroism analysis was performed on a JASCO J-600A spectropolarimeter. All the linear measurements were performed at room temperature in quartz cells of 1-mm path length.

2. Structures of the supramolecular complexes via MD simulations (Figs. S1-S2)

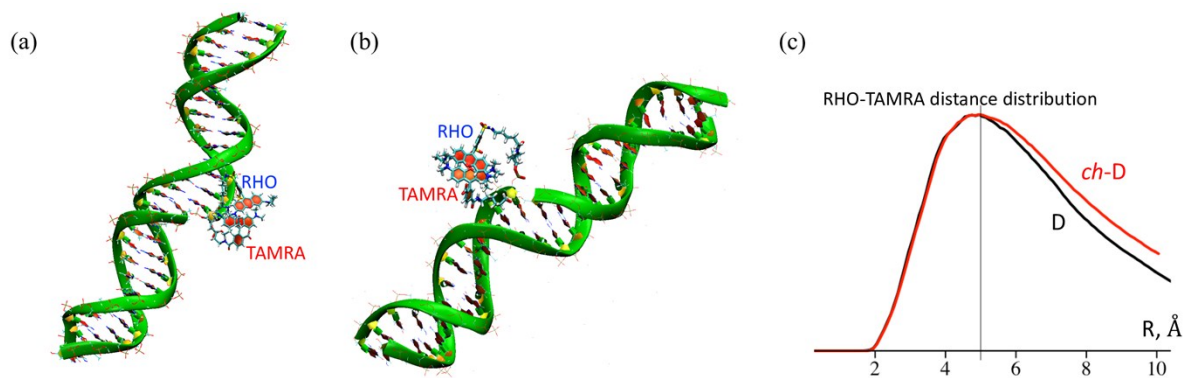


Fig. S1 Snapshots of the supramolecular complex of RHO and TAMRA chromophores in D (a) and *ch-D* (b) orientations tethered on a 23 base pair DNA strand from molecular dynamics simulations. Solvation box and counter-ions are shown in Fig. S2. (c) The distance distribution between the two units in the D (black line) and *ch-D* (red line) supramolecular complexes computed along MD trajectory.

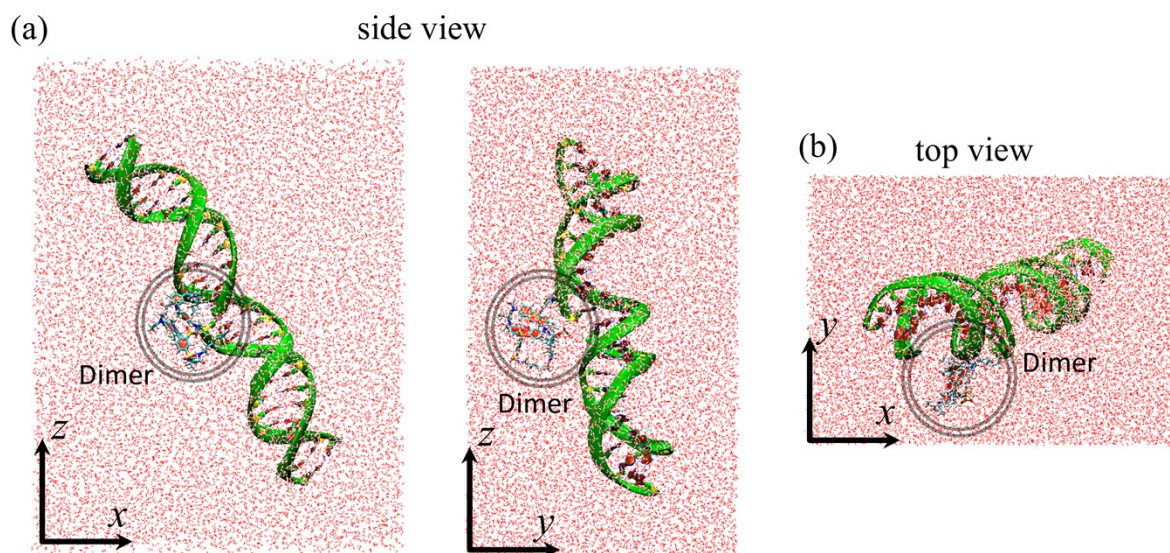


Fig. S2 Side (a) and top (b) view of the solvation periodic box for the supramolecular complex of RHO and TAMRA chromophores in *ch-D* orientation tethered on a 23 base pair DNA strand from molecular dynamics simulations. A rectangular box with side lengths of $91 \times 69 \times 112 \text{ \AA}$ was used.

3. Solvation shells for RHO and TAMRA units from MD simulations (Fig. S3)

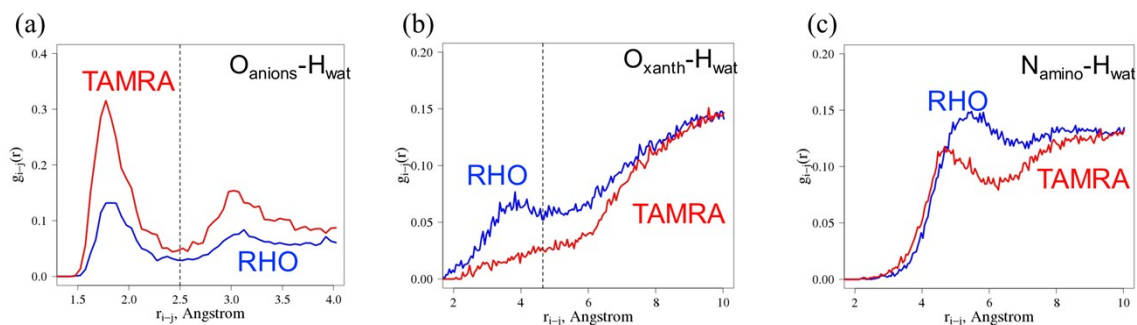


Fig. S3 Radial distribution functions, $g_{i-j}(r)$, relating two interacting centers i and j for RHO (blue) and TAMRA (red) for the 8 ns MD trajectory of the D conformer. Dashed lines denote the frontiers of the first minima of the function. (a) i : oxygen atoms of the anionic groups of the phenyl substituents, j : hydrogen atoms of the water molecules; (b) i : oxygen atoms of the xanthene moieties, j : hydrogen atoms of the water molecules; (c) i : nitrogen atoms of the amino-groups in the xanthene moieties, j : hydrogen atoms of the water molecules.

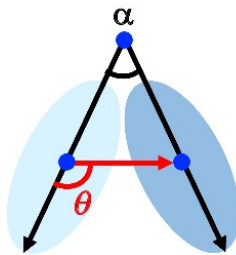
We analyze radial distribution functions along MD trajectory to identify specific contacts of heteroatoms of the chromophore with solvent molecules. The first solvation shell lies within the sphere of radius 2.5\AA from oxygen atoms of both anionic groups (see Fig. S3a). Solvation shells of the other heteroatoms are located at distances larger than 4\AA (Fig. S3b-c), hence we did not take them explicitly into account. The effect of the bulk water molecules was described using continuum solvation model (dielectric constant $\epsilon = 78.35$). We neglect the solvation effect of the DNA, which has lower dielectric constant, and of the ion concentration (HEPES buffer). The major effect on the electronic structure of the chromophore is expected to be governed by the polar water medium.

4. Intermolecular angles and coupling between the monomers (Fig. S4)

Following Kasha the coupling between the monomeric subunits can be written as:

$$\beta = \frac{1}{4\pi\epsilon_0} \left(\frac{\vec{\mu}_A \cdot \vec{\mu}_B}{r_{AB}^3} - 3 \frac{(\vec{\mu}_A \cdot \vec{r}_{AB})(\vec{\mu}_B \cdot \vec{r}_{AB})}{r_{AB}^5} \right) \quad (\text{S1})$$

where $\vec{\mu}_A$ and $\vec{\mu}_B$ are S₀-S₁ transition dipoles for each of the monomers and \vec{r}_{AB} is a vector connecting the molecular centers of A and B. If the vectors of the transition dipole are directed along the long xanthene axis, the dot product between the two dipoles $\vec{\mu}_A \cdot \vec{\mu}_B$ will depend on the angle between these vectors, angle α (Scheme S1). Each of the dot products $(\vec{\mu}_A \cdot \vec{r}_{AB})$ and $(\vec{\mu}_B \cdot \vec{r}_{AB})$ depends on the angle between the dipole and the \vec{r}_{AB} vector, angle θ (Scheme S1).



Scheme S1. Intermolecular angles α and θ that affect the coupling strength β in the dimer.

The composition of the states of the dimer $|\Psi_1\rangle$ and $|\Psi_2\rangle$ and the corresponding transition dipoles from the ground state $\vec{\mu}_1$ and $\vec{\mu}_2$ can be written as:

$$\begin{aligned} |\Psi_1\rangle &= \cos \xi |\Psi_A^* \Psi_B\rangle - \sin \xi |\Psi_A \Psi_B^*\rangle \\ |\Psi_2\rangle &= \sin \xi |\Psi_A^* \Psi_B\rangle + \cos \xi |\Psi_A \Psi_B^*\rangle \\ \vec{\mu}_1 &= \vec{\mu}_A \cos \xi - \vec{\mu}_B \sin \xi \\ \vec{\mu}_2 &= \vec{\mu}_A \sin \xi + \vec{\mu}_B \cos \xi \end{aligned} \quad (\text{S2})$$

where the mixing angle ξ is defined in the following way:

$$\tan 2\xi = \frac{2\beta}{E_A - E_B} \quad (\text{S3})$$

One can write the coupling strength in terms of the intermolecular angles:

$$\beta = \frac{\mu_A \mu_B}{4\pi\epsilon_0 r_{AB}^3} (\cos \alpha - 3 \cos^2 \theta) \quad (\text{S4})$$

An additional intermolecular angle is needed in order to estimate the order of the exchange interaction between the units, as we consider dimers with rather short distances (3-5 Å) between the monomeric centers. We call this angle γ , the angle between the normal vectors to the planes defined for each unit. In each unit, RHO and TAMRA, we define a local plane using 3 neighbouring carbon atoms C_1 , C_2 and C_3 (see Fig. S4). The normal vector \mathbf{n} is computed as a cross product of the two direction vectors on the plane, C_1-C_2 and C_1-C_3 . This allows us to find the coefficients of the plane (A, B, C, D) and to check if the next neighbouring atom C_4 also belongs to the same plane.

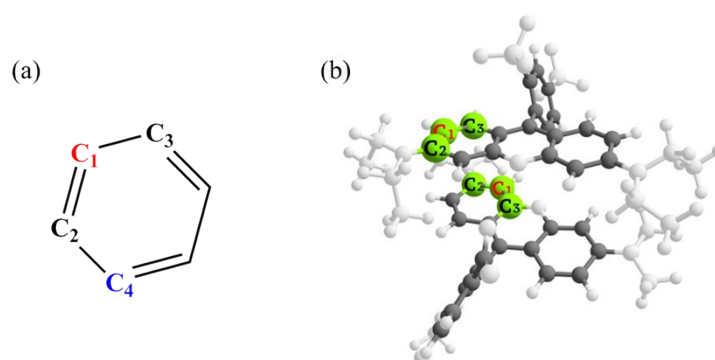


Fig. S4 Definition of the local planes in the xanthene moieties. (a) Each local plane is defined for 3 carbon atoms: C_1 and its near neighbours C_2 and C_3 . The fourth carbon atom C_4 , the nearest neighbour of C_2 , is used to verify that dihedral angle between the 4 atoms of the benzene ring is small. (b) An example of the set of 3 atoms in each TAMRA and RHO units used to define the local planes.

The γ_k angle between the normal vectors to the k pair of RHO and TAMRA local planes is computed directly via the dot product between the two normals:

$$\cos \gamma_k = \frac{\mathbf{r}_R^k \cdot \mathbf{r}_T^k}{\left(\sqrt{(A_R^k)^2 + (B_R^k)^2 + (C_R^k)^2} \right) \left(\sqrt{(A_T^k)^2 + (B_T^k)^2 + (C_T^k)^2} \right)} = \frac{A_R^k A_T^k + B_R^k B_T^k + C_R^k C_T^k}{\left(\sqrt{(A_R^k)^2 + (B_R^k)^2 + (C_R^k)^2} \right) \left(\sqrt{(A_T^k)^2 + (B_T^k)^2 + (C_T^k)^2} \right)} \quad (\text{S5})$$

where (A_R^k, B_R^k, C_R^k) and (A_T^k, B_T^k, C_T^k) are coefficients of the k pair of planes for RHO and TAMRA respectively. The averaged value γ is taken as $\gamma = \frac{1}{N} \sum_k \gamma_k$. For coplanar

conformations the γ angle is small and the whole complex has efficient π stacking interaction, therefore the dimer is more stable. In the present work we compute the optical properties of the

dimer at the ab initio level, therefore these angles are used only for qualitative comparison of the geometries of the two enantiomers and their calculated profiles.

5. Averaging of the profiles

The absorption lineshape averaged over the ensemble is built using excitation energies $\Delta E_{0b}(\mathbf{R}_l)$ and oscillator strengths $f_{0b}(\mathbf{R}_l)$ for the transitions from ground state to the low-lying excited states at the geometry \mathbf{R}_l of the chromophore. The absorption profile $\sigma_{0b}(E)$, as a function of energy, E , is modelled using the following expression:

$$\sigma_{0b}(E) = \frac{\pi \hbar e^2}{2mc\epsilon_0 n_r E} \frac{1}{N_s} \sum_{l=1}^{N_s} \Delta E_{0b}(\mathbf{R}_l) f_{0b}(\mathbf{R}_l) g_{Gauss}(E - \Delta E_{0b}(\mathbf{R}_l), \delta) \quad (\text{S5})$$

for the $0 \rightarrow b$ transitions from ground to the b excited electronic state for N_s samples. Here ϵ_0 is the vacuum permittivity, c is the speed of light, and e and m are the electron charge and mass respectively. Contribution from each snapshot is taken with a broadening given by a Gaussian function $g_{Gauss}(E - \Delta E_{0b}(\mathbf{R}_l), \delta)$ centered at the position of the excitation energy, $\Delta E_{0b}(\mathbf{R}_l)$, with dispersion, δ , equal to 250 cm^{-1} for all the samples in the ensemble. The circular dichroism profiles are averaged in an analogous way.

6. Absorption and CD properties of the bare dimers in solution (Table S1 and Fig. S5)

Table S1. Effect of the basis set on the relative energies in the ground state (GS) equilibrium geometry, δE (GS), excitation energies, E , oscillator strength of the absorption, f , and rotatory strength, CD, for conformations of the two isomers D and *ch*-D with left and right polarization of the first excitation. Relative energies, δE (GS), calculated in the 6-311G(d,p) basis are shown in brackets.

	6-311G(d,p)			6-311G++(d,p)		
	E , eV	f	CD	E , eV	f	CD
<i>ch</i> -D/PCM, δE (GS) = 0 kcal/mol						
S ₀ -S ₁	2.58	0.57	-157.0	2.57	0.54	-169.3
S ₀ -S ₂	2.78	1.94	184.9	2.76	2.01	197.8
D/PCM, δE (GS) = 0.04 (0.06) kcal/mol						
S ₀ -S ₁	2.58	0.58	152.1	2.57	0.55	164.2
S ₀ -S ₂	2.78	1.94	-180.9	2.76	2.00	-194.8

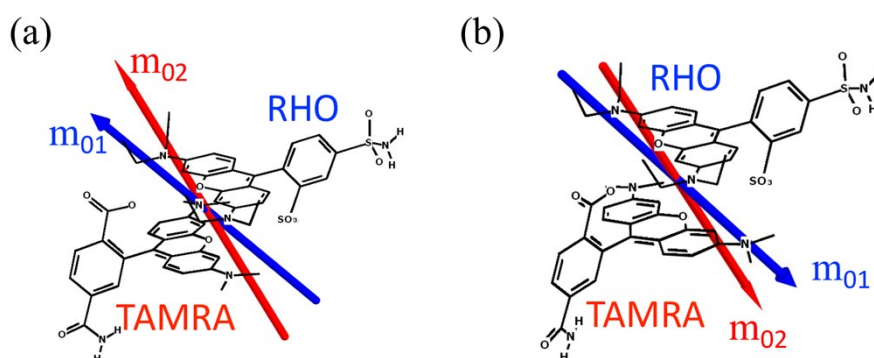


Fig. S5 Vectors of the magnetic transition dipoles. Vectors of the magnetic transition dipoles for the first (blue arrows) and second (red arrows) transitions in the D (a) and *ch*-D (b) bare dimers. The CD sign of the S₀-S₁ transition for the D orientation is positive, while for the *ch*-D orientation it is negative as obtained within TDDFT/PCM calculations. The sign for the second transition is opposite to the sign of the first, which is expected for two coupled monomers.

7. Distributions for the intermolecular angles in the D and *ch*-D isomers
(Figs. S6-S7)

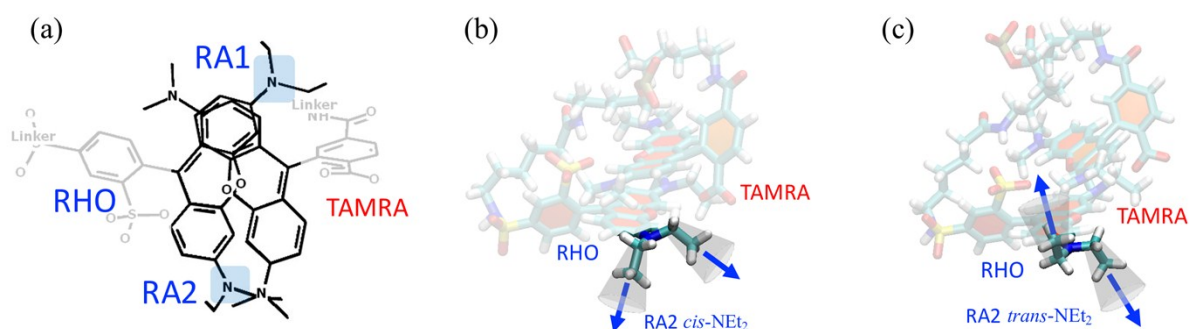


Fig. S6 (a) Definition of the RA1 and RA2 ethyl-amino-groups of RHO, NEt₂, in the D form of heterodimer. In the oblique orientation RA1 amino-group of RHO is the one closest to the TAMRA, while the RA2 amino-group is further away. The RA1 and RA2 amino-groups in the chiral *ch*-D enantiomer are defined in similar way. (b, c) An example of RA2 amino-group in *cis* (b) and *trans* (c) conformations. *Cis-trans* transformation of these amino-groups affects the π stacking coplanar geometry of the dimer.

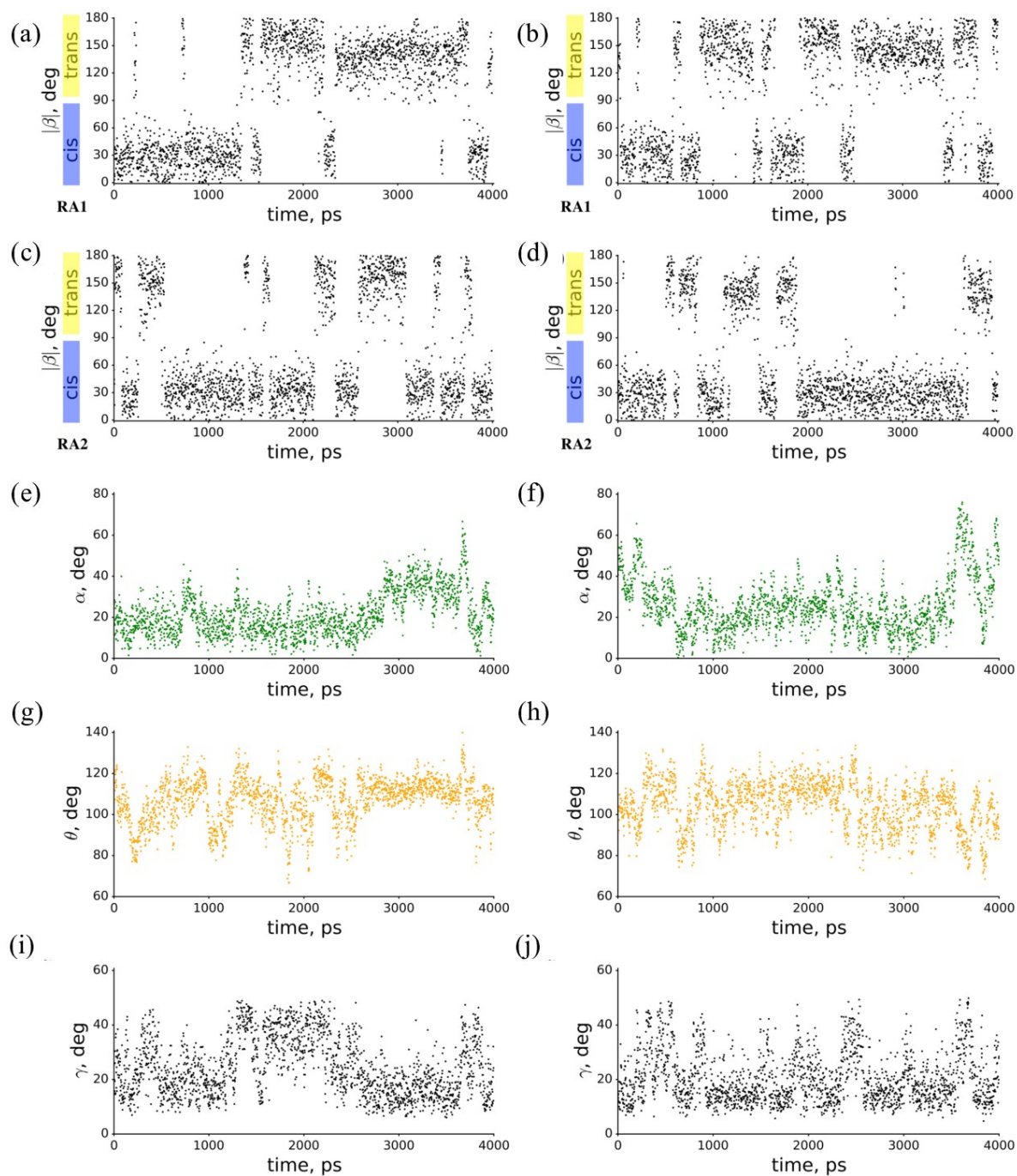


Fig. S7 Change in the conformation of the RHO amino-group RA1 (a,b) and RA2 (c,d) and intermolecular angles along MD trajectory in D (a, c, e, g, i) and *ch*-D (b, d, f, h, j) enantiomers. The conformations are determined via the dihedral angle β between the two ethyls of the amino-group: angles lower than 90° correspond to the *cis*-conformation, larger than 90° to the *trans*-conformation. (e, f) the angle, α , between the long axes of the monomers; (g, h) the angle, θ between the long axis of RHO and line connecting the molecular centers in the RHO \rightarrow TAMRA direction; (i, j) the angle, γ between the normal vectors to RHO and TAMRA xanthene planes.

8. Typical structure for the excited state computation (Fig. S8)

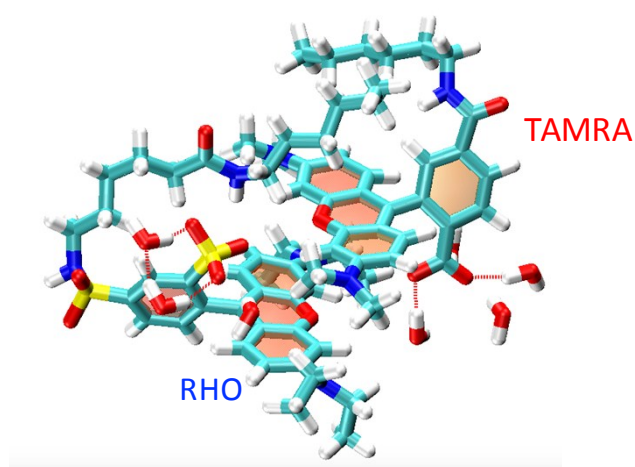


Fig. S8 Snapshot of a typical geometry used in the excited state TDDFT/PCM calculations for the ensemble of the geometries sampled during 4 ns MD trajectory of the D conformer. Chromophores and nearest linker atoms are taken into account with specific solvation around anionic sulfo- and carboxy-groups (water molecules within the distance less than 2.5\AA from heteroatoms).

9. The dominant natural transition orbital pairs (Fig. S9)

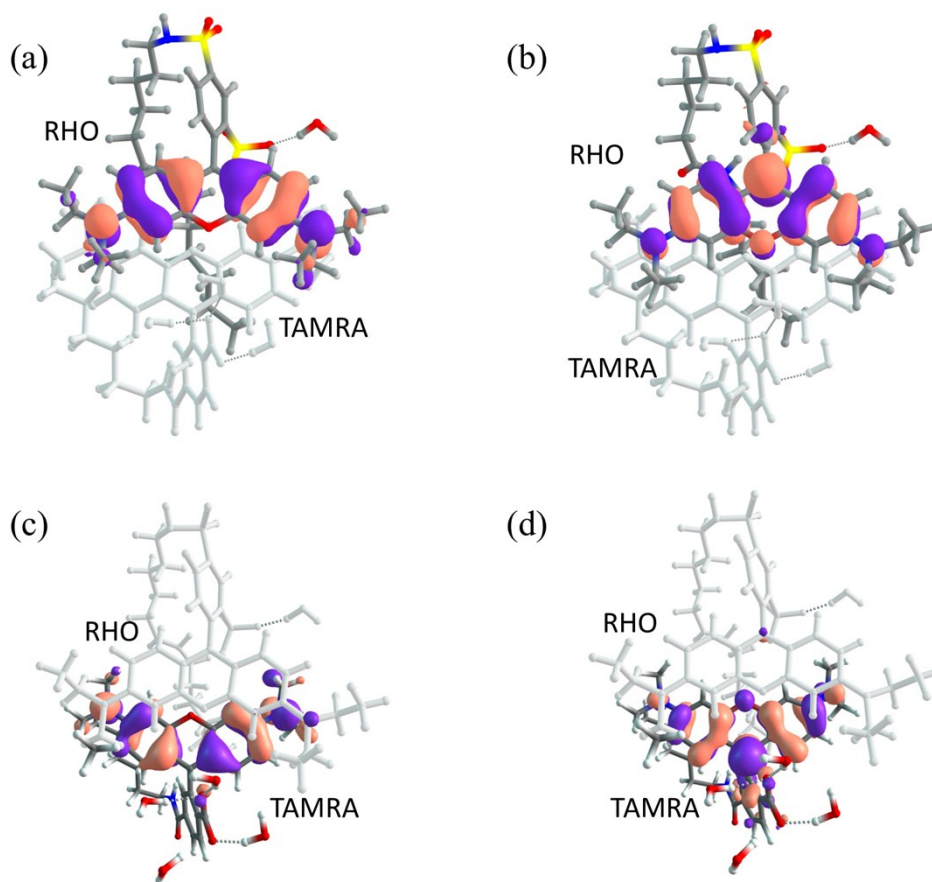


Fig. S9 The dominant natural transition orbital pairs for the S_0 - S_1 (a, b) and S_0 - S_2 (c, d) transitions of the D dimer: (a, c) the “hole” NTOs, (b, d) the “particle” NTOs. The weight ω is 0.89 and 0.91 for S_0 - S_1 and S_0 - S_2 transitions respectively, which corresponds to a localized character of the transition.

10. Structures with spurious electronic transitions

In 11% for D and 8% for *ch*-D conformer of all the samples, the second electronic transition is localized on RHO. In this case the first transition localized on TAMRA has a smaller intensity than the second. Reversing the localization of the states on the subunits therefore does not affect which transition has the brightest character, in both cases, it is the second one. Since the change of the localization of the two lowest transitions might arise from a strong distortion of the geometry snapshot, we do not take into account these spurious samples. In the group of samples with delocalized transitions there are structures (13% and 10% of the whole ensemble for D and *ch*-D) for which the two bands in the absorption spectrum lie within a gap smaller than 0.1 eV (less than 800 cm⁻¹, Figs. S10-S11(c-d) of the SI). These small gaps are far smaller than the accuracy of TDDFT energies therefore we do not include them in the average spectrum. In the rest, 4.75% for D and 6.75% for *ch*-D of samples, the two lowest states are pure charge-transfer (CT) states which are not accurately described at the TDDFT level. We also exclude them for building the average absorption and CD spectra.

11. Spectra averaged over localized and delocalized transitions (Figs. S10-S13)

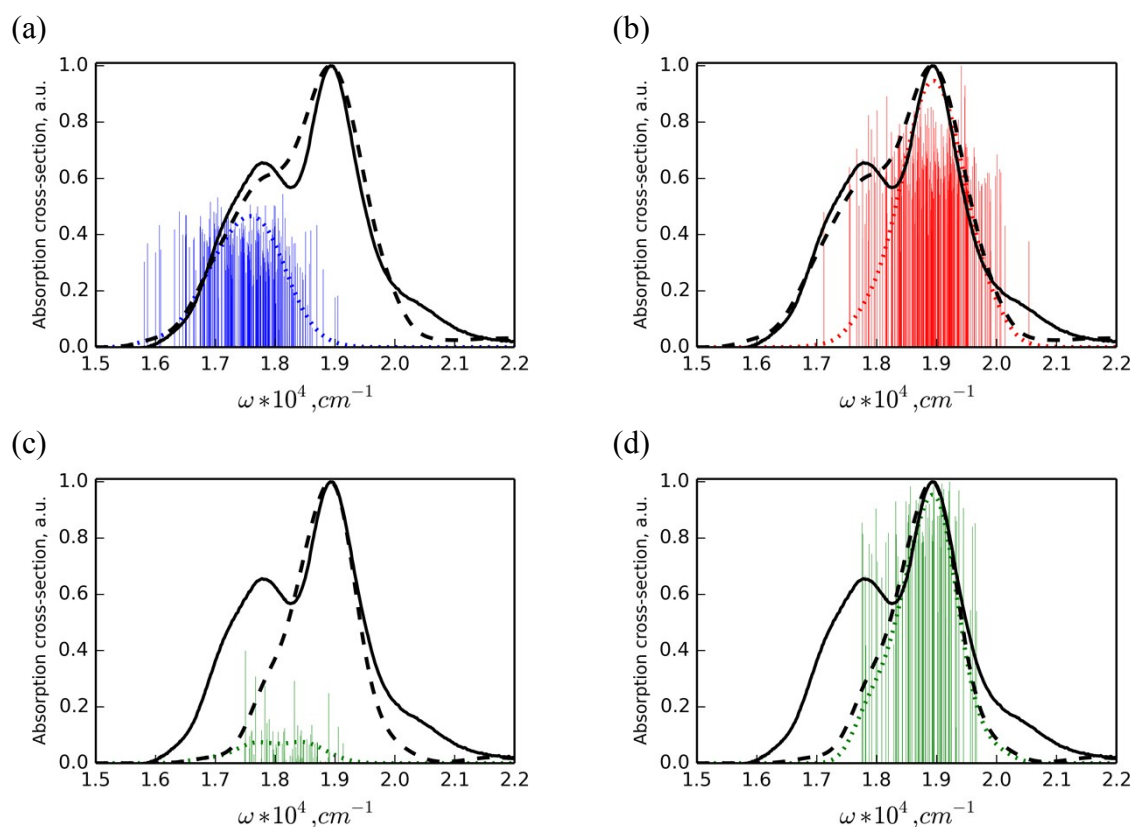


Fig. S10 Experimental (black solid line) and calculated (black dashed line) absorption lineshapes for the groups of samples with localized (255 samples, a-b) and delocalized (25 samples, c-d) transitions computed for the D enantiomer. The partial contribution for the S_0-S_1 (a, c) and S_0-S_2 (b, d) transitions is shown as sticks and their average profile as a dashed line of the same color. The profiles are built up with same Gaussian broadening for all transitions. The intensity of each spectrum is scaled to its maximum. The calculated profiles are shifted to the positions of the experimental maxima by -584 cm^{-1} .

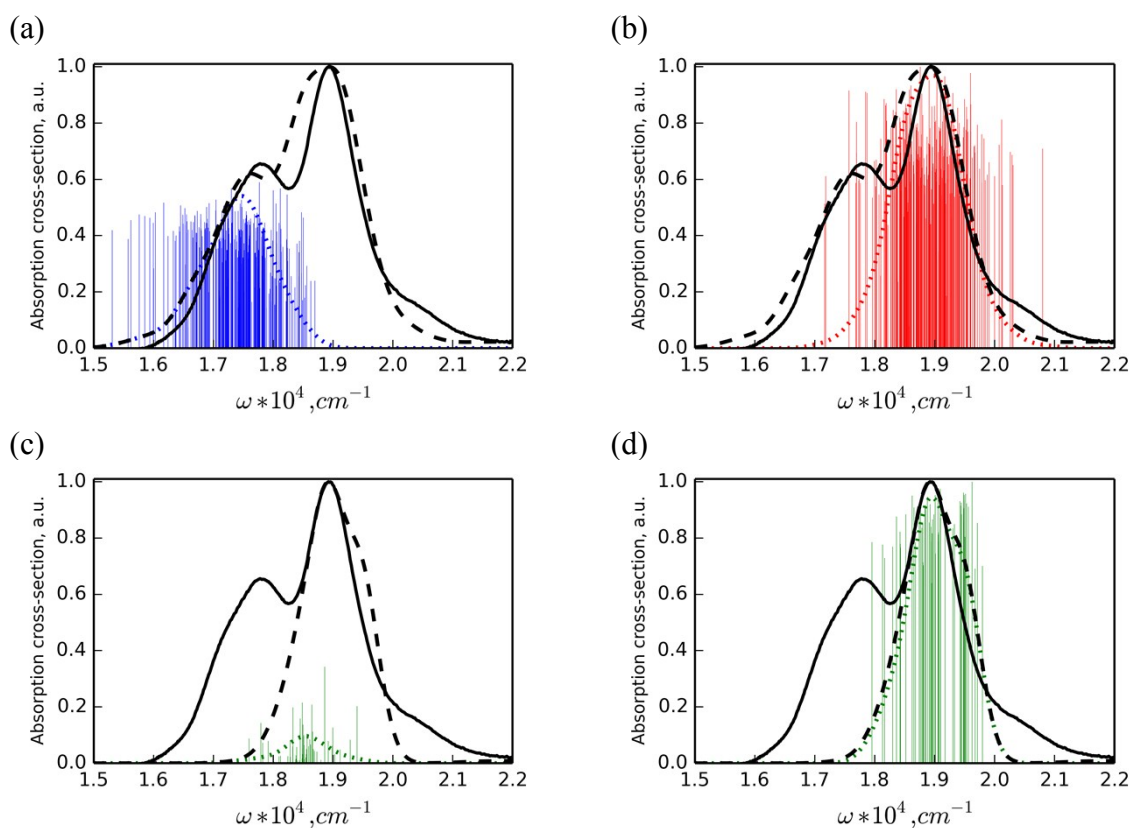


Fig. S11 Experimental (black solid line) and calculated (black dashed line) absorption lineshapes for the groups of samples with localized (280 samples, a-b) and delocalized (25 samples, c-d) transitions only. The calculated profiles correspond to the samples of the *ch*-D optical isomer. The partial contribution for the S_0 - S_1 (a, c) and S_0 - S_2 transitions (b, d) is shown as sticks and their average profile as a dashed line of the same color. The profiles are built up with same Gaussian broadening for all transitions. The intensity of each spectrum is scaled to its maximum. The calculated profiles are shifted down to the positions of the experimental maxima by -713 cm^{-1} .

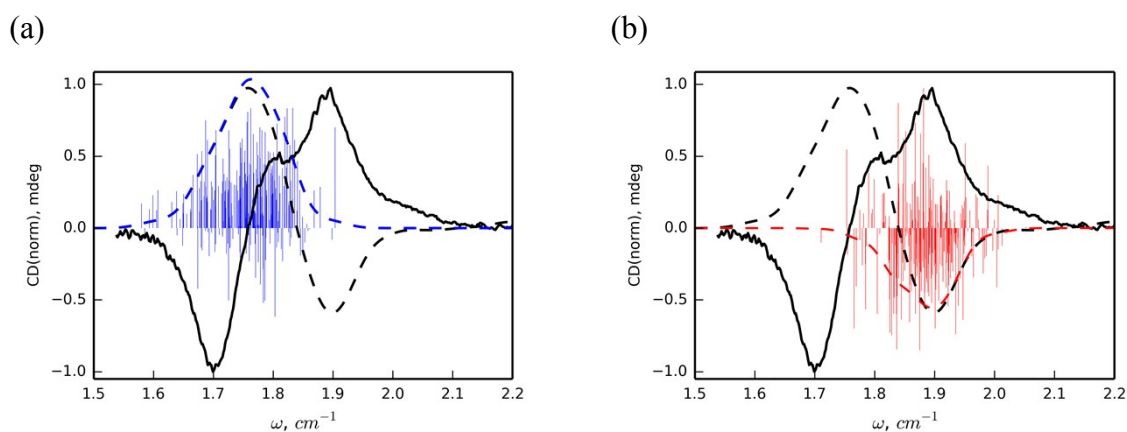


Fig. S12 Experimental CD spectrum (solid line) and calculated CD signal (black dashed line) for the group with localized transitions only (255 samples) in the D isomer. Sticks refer to the position and intensity of the transition in each sample: (a) S_0 - S_1 excitation in blue colour, (b) S_0 - S_2 in red colour. The dashed line of the same colour corresponds to the partial contribution of the specific excitation, S_0 - S_1 or S_0 - S_2 , to the overall spectrum.

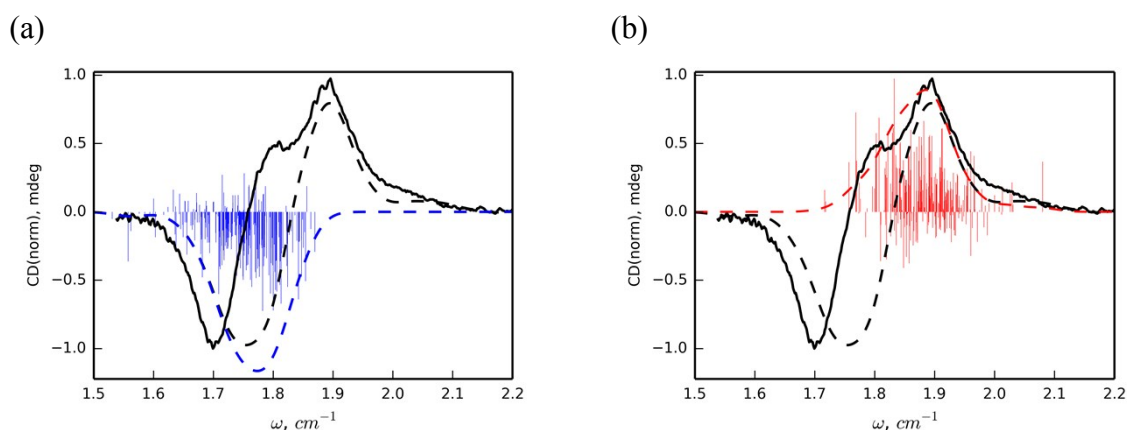


Fig. S13 Experimental CD spectrum (solid line) and calculated CD signal (dashed line) for the group with localized transitions only (280 samples) in the *ch*-D isomer. Sticks refer to the position and intensity of the transition in each sample: (a) S_0 - S_1 excitation in blue colour, (b) S_0 - S_2 in red colour. The dashed line of the same colour corresponds to the partial contribution of the specific excitation, S_0 - S_1 or S_0 - S_2 , to the overall spectrum.

12. Oscillator strength for the S_0 - S_1 transition (Fig. S14)

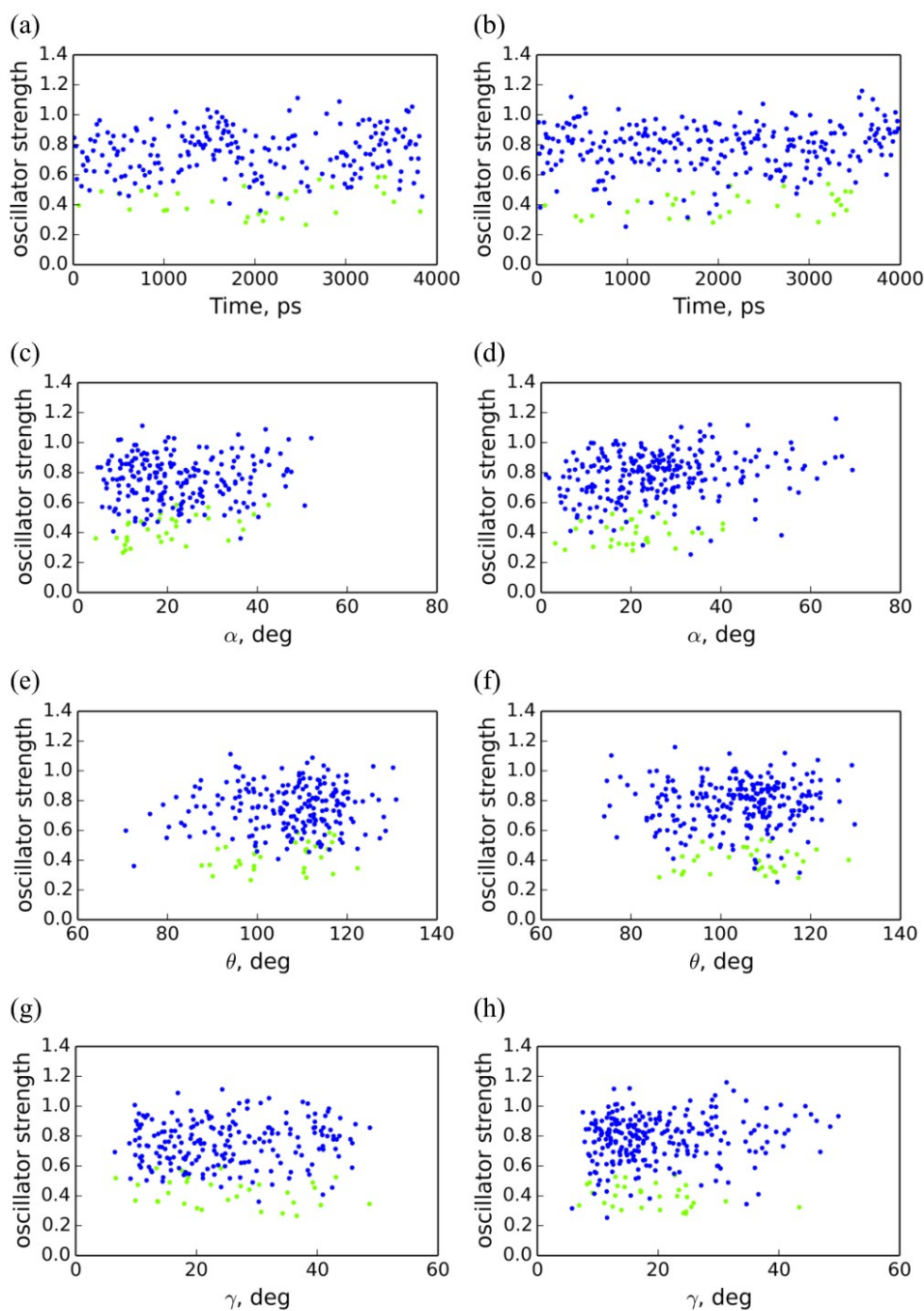


Fig. S14 Correlation between the intermolecular angles and oscillator strength of the S_0 - S_1 transition for D (a,c,e,g) and *ch*-D (b,d,f,h) enantiomers. The color of the dots denote the weight ω of the NTO of the RHO unit, green: $\omega = 0.8-0.9$, blue dots: $0.9-1$. See Fig. 2 for the definition of the angles. No clear correlation with one specific angle is observed. However lower oscillator strength is characteristic to larger delocalized transition.

13. Scheme of the optical isomerisation

Scenario of the *ch*-D isomerisation

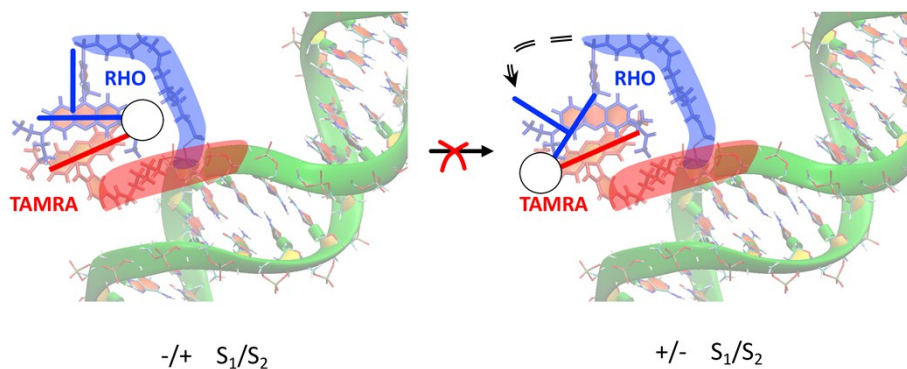


Fig. S15. Scheme for the isomerisation of the *ch*-D dimer into its optical isomer. RHO and TAMRA chromophores are shown in blue and red color, respectively. The long axes of the RHO and TAMRA xanthenes are shown schematically as lines of the respective color. One can see that the length of the RHO linker should be longer for this transformation to be present (highlighted with a black dashed arrow).

14. Table of the coordinates of the bare dimers

Equilibrium geometry of the ground state for the D dimer (124 atoms) in xyz-format:

124

D-form, +/- S1/S2

6	0.395312	2.951804	1.504773
6	1.309038	1.972513	1.302648
6	0.964396	0.597476	1.411135
6	-0.389009	0.316679	1.732203
6	-1.336284	1.283394	1.920389
6	-0.976711	2.642233	1.799566
6	1.851799	-0.458385	1.234727
6	0.052708	-2.000635	1.740193
6	1.406041	-1.775386	1.413179
6	2.217581	-2.927722	1.277024
1	3.260635	-2.804143	1.019504
6	1.719016	-4.177894	1.460387
6	0.339723	-4.390347	1.788960
6	-0.473478	-3.252963	1.937589
1	0.711164	3.979499	1.422332
1	2.327556	2.234279	1.052336
1	-2.350128	0.956794	2.110877
1	2.384172	-5.019540	1.352548
1	-1.521120	-3.316985	2.181993
8	-0.803155	-0.964504	1.871020
6	3.291982	-0.195082	0.964395
6	4.144126	-0.125253	2.065711
6	3.813063	-0.027023	-0.317743
6	5.496791	0.107961	1.901746
1	3.736635	-0.254919	3.059965
6	5.169611	0.201828	-0.491680
6	5.991866	0.266863	0.617211
1	6.153346	0.169095	2.759019
1	5.565622	0.327652	-1.489148
16	7.732138	0.560283	0.393263
8	8.211979	1.388462	1.489246
8	7.926907	1.004614	-0.978644
7	8.382310	-0.938273	0.647682
1	8.386797	-1.516897	-0.185428
7	-0.159496	-5.636729	1.936153
7	-1.892673	3.615123	1.939642
6	-1.543308	-5.839841	2.365357
1	-2.194600	-5.181292	1.787860
1	-1.816191	-6.857493	2.090437
6	0.680800	-6.825066	1.780794
1	0.017215	-7.649541	1.523005
1	1.336657	-6.687002	0.921129

6	-1.767099	-5.631290	3.859188
1	-1.473362	-4.628500	4.171688
1	-2.824726	-5.763659	4.094246
1	-1.195297	-6.351571	4.444708
6	1.490412	-7.179627	3.022703
1	2.114005	-8.052422	2.820489
1	2.142253	-6.357192	3.321376
1	0.836870	-7.417324	3.862557
6	-3.288093	3.283568	2.244344
1	-3.569351	2.404247	1.670504
1	-3.899135	4.107793	1.878196
6	-1.527950	5.031080	1.884502
1	-2.440460	5.580071	1.656980
1	-0.856208	5.192464	1.041216
6	-3.558053	3.037166	3.723520
1	-4.570376	2.646782	3.835057
1	-2.869336	2.291074	4.123835
1	-3.456948	3.950207	4.311844
6	-0.914887	5.560837	3.175382
1	-0.006264	5.017122	3.438183
1	-0.657544	6.614860	3.055778
1	-1.615434	5.472833	4.006210
1	9.302442	-0.867948	1.069245
16	2.771950	-0.060312	-1.791476
8	3.716460	-0.106520	-2.921009
8	1.996445	1.193532	-1.731726
8	1.956827	-1.281269	-1.655760
6	-8.227394	-0.118563	-0.865771
6	-7.541197	0.126756	0.308175
6	-6.151158	0.121682	0.341745
6	-5.447297	-0.125632	-0.836023
6	-6.137806	-0.357967	-2.022341
6	-7.527339	-0.350911	-2.045721
1	-9.308967	-0.132941	-0.890567
1	-8.063891	0.325667	1.234225
1	-5.572019	-0.567134	-2.921948
6	-3.960189	-0.122237	-0.912773
6	-3.249151	-1.330552	-0.987575
6	-3.270658	1.080382	-1.143381
6	-3.823424	-2.613690	-0.808917
6	-1.864313	-1.303285	-1.260793
6	-1.879228	1.046031	-1.372091
6	-3.869517	2.364484	-1.143472
6	-3.084649	-3.749846	-0.926919
1	-4.878567	-2.682283	-0.580239
6	-1.093812	-2.432184	-1.394880
6	-1.111606	2.168101	-1.567053

1	-4.937407	2.441351	-0.988247
6	-3.134798	3.494447	-1.324786
6	-1.687121	-3.694848	-1.235435
1	-3.570091	-4.704663	-0.796904
1	-0.042336	-2.290241	-1.600554
6	-1.717606	3.432235	-1.516712
1	-0.051853	2.020016	-1.719804
1	-3.635441	4.450081	-1.314133
6	-5.415722	0.356806	1.656495
8	-6.086733	0.754796	2.622681
8	-4.182984	0.122925	1.614882
8	-1.219085	-0.129713	-1.418448
6	-8.318071	-0.619737	-3.290942
8	-9.470110	-1.022637	-3.231964
7	-0.958840	-4.823587	-1.369025
7	-0.983428	4.562170	-1.641225
6	-1.633657	5.856793	-1.786193
1	-2.293872	6.062504	-0.943464
1	-0.869970	6.629258	-1.804744
1	-2.214884	5.920440	-2.711224
6	0.430708	4.471900	-1.977197
1	0.882639	5.453130	-1.858873
1	0.942962	3.776816	-1.313869
1	0.580000	4.136401	-3.009082
6	0.415534	-4.739765	-1.841514
1	0.860188	-5.730468	-1.810555
1	0.462431	-4.365891	-2.869330
1	1.007635	-4.080978	-1.207421
6	-1.592192	-6.132966	-1.326375
1	-2.256417	-6.293250	-2.181143
1	-0.818620	-6.895381	-1.342585
1	-2.166540	-6.263407	-0.409777
7	-7.687175	-0.401699	-4.465207
1	-8.213374	-0.532676	-5.314672
1	-6.823560	0.110318	-4.522472

ch-D dimer:

124

ch-D-form, -/+ S1/S2

6	2.469739	3.783723	1.046891
6	2.919078	2.507335	0.929692
6	2.079997	1.396204	1.187817
6	0.753233	1.690503	1.565339
6	0.277385	2.971131	1.698722
6	1.116471	4.066148	1.426832
6	2.474098	0.055282	1.079270

6	0.238072	-0.605376	1.737183
6	1.563714	-0.954571	1.370275
6	1.857761	-2.345148	1.337809
1	2.853208	-2.658778	1.056231
6	0.924253	-3.275926	1.649109
6	-0.420480	-2.899254	1.988456
6	-0.729439	-1.523457	2.034916
1	3.154399	4.592305	0.847088
1	3.943069	2.329995	0.630620
1	-0.753664	3.089329	1.989227
1	1.201837	-4.317440	1.619514
1	-1.721245	-1.149592	2.252755
8	-0.126581	0.696123	1.811057
6	3.889553	-0.273743	0.755810
6	4.798101	-0.287374	1.813002
6	4.337401	-0.542376	-0.537135
6	6.134095	-0.570314	1.596386
1	4.449380	-0.070158	2.814343
6	5.676619	-0.819574	-0.764343
6	6.555409	-0.831202	0.302557
1	6.837722	-0.573010	2.417708
1	6.018450	-1.005208	-1.772466
16	8.273115	-1.188824	0.008239
8	9.078536	-0.434016	0.956223
8	8.512722	-1.032617	-1.418629
7	8.393354	-2.769591	0.478307
1	8.131214	-3.421587	-0.253404
7	-1.358791	-3.828064	2.237454
7	0.664097	5.336250	1.506009
6	-2.727816	-3.428885	2.578403
1	-3.004641	-2.577621	1.961974
1	-3.381138	-4.251806	2.290752
6	-1.040833	-5.256124	2.267926
1	-1.981133	-5.788309	2.132422
1	-0.423358	-5.501545	1.403541
6	-2.924909	-3.081626	4.048613
1	-2.194787	-2.337460	4.371878
1	-3.917764	-2.648665	4.176651
1	-2.828609	-3.959473	4.689074
6	-0.372026	-5.711579	3.559563
1	-0.155790	-6.780140	3.505655
1	0.567045	-5.183423	3.731080
1	-1.021097	-5.537560	4.418180
6	-0.685251	5.618397	1.996080
1	-1.390483	4.947288	1.502292
1	-0.939438	6.625012	1.667753
6	1.527940	6.479909	1.209508

1	0.875222	7.301167	0.915915
1	2.134106	6.249526	0.333282
6	-0.828808	5.518486	3.510776
1	-1.866021	5.705283	3.794708
1	-0.550777	4.528761	3.874851
1	-0.200433	6.254873	4.012250
6	2.411165	6.909319	2.375136
1	3.056191	6.094195	2.706885
1	3.045794	7.743425	2.070077
1	1.809752	7.234085	3.224746
1	9.315528	-2.967183	0.852759
16	3.221843	-0.573528	-1.955642
8	4.106730	-0.652889	-3.130683
8	2.461603	0.687149	-1.875062
8	2.402963	-1.785078	-1.759867
6	-7.715082	-0.164409	-0.498388
6	-6.974460	-0.331669	0.656074
6	-5.584313	-0.329868	0.624468
6	-4.936745	-0.170017	-0.599999
6	-5.682072	0.005281	-1.762659
6	-7.071095	0.022094	-1.717625
1	-8.796781	-0.171591	-0.476310
1	-7.453526	-0.470102	1.616035
1	-5.159695	0.097119	-2.707130
6	-3.456738	-0.227250	-0.753379
6	-2.816238	-1.464624	-0.935908
6	-2.715617	0.949477	-0.946852
6	-3.451722	-2.725851	-0.819589
6	-1.438249	-1.491294	-1.236530
6	-1.348166	0.858537	-1.285430
6	-3.241457	2.260124	-0.827792
6	-2.761140	-3.888765	-0.961722
1	-4.511646	-2.757347	-0.605203
6	-0.715312	-2.648270	-1.393659
6	-0.552137	1.949664	-1.533848
1	-4.280700	2.378681	-0.551708
6	-2.476238	3.360750	-1.059588
6	-1.354598	-3.885857	-1.228127
1	-3.288495	-4.824620	-0.860989
1	0.338789	-2.545399	-1.609297
6	-1.098766	3.239069	-1.432890
1	0.482591	1.759609	-1.781416
1	-2.925630	4.337673	-0.970397
6	-4.788932	-0.486348	1.916418
8	-5.419823	-0.797249	2.939997
8	-3.555362	-0.284657	1.800079
8	-0.747250	-0.343469	-1.394981

6	-7.919170	0.194511	-2.942005
8	-9.074432	-0.202311	-2.971233
7	-0.661137	-5.044737	-1.312346
7	-0.345579	4.331501	-1.680880
6	-0.938260	5.660338	-1.700893
1	-1.457837	5.874220	-0.767459
1	-0.145739	6.394588	-1.813844
1	-1.643446	5.780305	-2.529042
6	0.999967	4.170706	-2.212676
1	1.475349	5.145766	-2.269878
1	1.603358	3.535169	-1.565615
1	0.983507	3.729032	-3.214206
6	0.738349	-5.022680	-1.714642
1	1.168654	-6.005567	-1.541735
1	0.850261	-4.769490	-2.774392
1	1.298555	-4.296267	-1.128213
6	-1.356282	-6.323785	-1.345520
1	-1.989574	-6.420686	-2.232635
1	-0.618134	-7.120777	-1.360366
1	-1.974697	-6.459655	-0.458016
7	-7.334884	0.799535	-3.998921
1	-7.898709	0.968528	-4.816954
1	-6.466128	1.299148	-3.916075